Kinematics of swimming of the manta ray: three-dimensional analysis of open water maneuverability

Frank E. Fish[1,*], Allison Kolpas[2], Andrew Crossett[2], Michael A. Dudas[3], Keith W. Moored[4] and Hilary Bart-Smith[5]

[1]Department of Biology, West Chester University, West Chester, PA 19383, USA

[2]Department of Mathematics, West Chester University, West Chester, PA 19383, USA

[3]Dudas' Diving Duds, West Chester, PA 19380, USA

[4]Department of Mechanical Engineering and Mechanics, Lehigh University, Bethlehem, PA 18015, USA

[5]Department of Mechanical and Aerospace Engineering, University of Virginia, Charlottesville, VA 22904, USA

*Author for correspondence (ffish@wcupa.edu)

Author for correspondence: Frank E. Fish

Address: Department of Biology, West Chester University. West Chester PA 19383, USA

Phone: (610)-436-2460

Abstract

For aquatic animals, turning maneuvers represent a locomotor activity that may not be confined to a single coordinate plane, making analysis difficult particularly in the field. To measure turning performance in a three-dimensional space for the manta ray (*Mobula birostris*), a large open-water swimmer, scaled stereo video recordings were collected. Movements of the cephalic lobes, eye and tail base were tracked to obtain three-dimensional coordinates. A mathematical analysis was performed on the coordinate data to calculate the turning rate and curvature (1/turning radius) as a function of time by numerically estimating the derivative of manta trajectories through three-dimensional space. Principal component analysis (PCA) was used to project the three-dimensional trajectory onto the two-dimensional turn. Smoothing splines were applied to these turns. These are flexible models that minimize a cost function with a parameter controlling the balance between data fidelity and regularity of the derivative. Data for 30 sequences of rays performing slow, steady turns showed the highest 20% of values for the turning rate and smallest 20% of turn radii were 42.65+16.66 deg s^{-1} and 2.05+1.26 m, respectively. Such turning maneuvers fall within the range of performance exhibited by swimmers with rigid bodies.

Summary Statement

Underwater stereovideography was used to detail the three-dimensional maneuvering performance of a large pelagic animal, the manta ray, in its natural environment.

INTRODUCTION

Unsteady swimming is a vital aspect of the locomotor repertoire of aquatic animals (Webb, 1997, 2006; Fish and Domenici, 2015). Unsteady motions are related to changes in speed, orientation, and direction (e.g., turning, acceleration). By utilizing self-induced instabilities (i.e., muscular effort), animals can produce changes in state of the center of mass and effect maneuvers. Maneuvers are important for catching prey, escape from predators, negotiating obstacles in complex spatial environments, avoiding environmental disturbances, and ritualistic displays and mating (Howland, 1974; Webb, 1976, Weihs and Webb, 1984, Domenici and Blake, 1997; Maresh et al., 2004; Walker, 2004; Ware et al., 2014; Fish and Hoffman, 2015). Turning has been the focus of the majority of research on maneuvers, particularly with respect to lateral or yawing turns (i.e., rotation around the vertical axis normal to the axis of motion; Walker, 2000; Webb, 1994, 2006).

Turning performance is assessed by measurements of maneuverability and agility. Maneuverability is the capability to turn in a confined space and is measured as length-specific radius of the turn trajectory (R/L, where R is the radius of the turn and L is total body length); agility is the rate of turn measured as the angular velocity (ω) (Norberg and Rayner, 1987; Webb, 1994; Walker, 2000). Norberg and Rayner (1987) considered an inverse relationship between maneuverability and agility, whereby an animal can turn tightly at a low speed or make a wide turn at higher speeds. However compared to large-bodied swimmers, swimmers of small size can be highly maneuverable and agile, because turning radius is proportional to body length and agility decreases with

increasing size (Webb, 1994; Fish and Nicastro, 2003; Parson et al., 2011). In addition, swimmers with greater flexibility of the body are more agile with high maneuverability than rigid-bodied animals of equal size (Fish, 2002; Fish and Nicastro, 2003; Parson et al., 2011).

The majority of studies of turning performance by marine vertebrates (e.g., fish, turtle, penguin, sea lion, dolphins) have been confined to animals, which were examined in laboratory or aquarium settings (Webb and Keyes, 1981; Webb, 1983; Hui, 1985; Blake et al., 1995; Webb et al., 1996; Domenici and Blake, 1997; Gerstner, 1999; Schrank et al., 1999; Walker, 2000; Webb and Fairchild, 2001; Fish et al., 2003, 2012; Domenici et al., 2004; Rivera et al, 2006; Cheneval et al., 2007; Danos and Lauder, 2007; Parson et al., 2011). In certain cases, these studies were able to determine maximal performance in terms of maneuverability and agility by manipulation of the test environment or through training. Unrestrained swimming by vertebrates in nature is difficult to examine due to factors such as infrequent observations, size of the animal, and difficulty setting up reliable recording equipment. Recently, the maneuvering performance has been recorded for large cetaceans by multi-sensor tags and underwater cameras that were mounted on the whales (Hazen et al., 2009; Ware et al., 2011, 2014; Wiley et al., 2011; Goldbogen et al., 2013; Williams et al. 2015). However, this new methodology has limitations due to the inability to accurately determine position and velocity, and to place the animal in a fixed frame of reference. As a result, measures of maneuverability and agility may not have the accuracy of direct observation. Furthermore, the association of kinematics of the mobile control surfaces (e.g., flukes, flippers) with the turning radius and rate are limited.

The use of three-dimensional videography provides the opportunity for enhanced accuracy and precision to examine maneuvering performance of aquatic animals (Boisclair, 1992; Hughes and Kelly, 1996). The swimming kinematics of the body and fins of fishes have been examined with three-dimensional videography for steady swimming and maneuvering (Boisclair, 1992; Tytell et al., 2008; Blevins and Lauder, 2012). However, these studies were performed in the laboratory in confined spaces. The only field studies using three-dimensional video tracking were for trout (*Salmo* sp.) that were foraging in a river (Boisclair, 1992; Hughes and Kelly, 1996; Hughes et al., 2003). The movements of relatively small (range 0.55-0.63 m) trout were examined to determine the swimming speeds and reaction volumes used to detect and acquire prey.

Mantas (*Mobula birostris and Mobula alfredi*; family Myliobatidae) are the largest of the over 500 elasmobranch species of batoid fishes (skates and stingrays), which have relatively rigid dorsoventrally compressed bodies and expanded pectoral fins (Rosenberger, 2001; Douady et al., 2003; Marshall et al., 2009; Kitchen-Wheeler, 2010). The manta can weigh over 1580 kg and is reported to have high aspect ratio (3.5, ratio of span to chord) pectoral fins that can reach a span of over 9 m (Perlmutter, 1961; Deacon et al., 1997; Compagno, 1999; Homma et al., 1997; Last and Stevens, 2009; Fontanella et al., 2013). Mantas use oscillatory locomotion (mobuliform mode) where there is a small undulatory component (the wavelength of the undulation is greater than the chord length of the pectoral fin), and swim primarily by flapping the pectoral fins dorsoventrally analogous to the flight of birds (Klausewitz, 1964; Webb, 1994; Rosenberger, 2001).

Mantas are able to execute turning maneuvers (Clark, 1969; Duffy and Abbott, 2003; Fish et al., 2012). The pectoral fins exhibit a range of both symmetrical and asymmetrical motions (Homma et al., 1997), which can assist in turning. Although capable of leaping behavior, the most notable swimming maneuver by manta is a looping or backward somersault behavior used in feeding and mating (Bigelow and Schroeder, 1953; Homma et al., 1999; Duffy and Abbott, 2003; Fish et al., 2012).

While swimming and maneuvering capabilities by the manta indicate a high level of performance (Homma et al., 1999; Duffy and Abbott, 2003; Fish et al., 2012), these studies were limited by the lack of quantitative measurements on maneuverability and agility. Furthermore, swimming performance has not been performed in the field. Previous work by Parson et al. (2011) on maneuvering rays was only performed on small species in an aquarium setting using a single camera. Data on maneuvering performance are limited if video recordings are taken with a single camera and the animal swims outside the focal plane of the camera. The size of the manta and its operation within a large three-dimensional space present a challenge to measure turning capabilities in open water. In this study, we quantitatively analyzed the trajectory of the manta with stereovideography underwater to detail the three-dimensional maneuvering performance in its natural environment. This is the first time that the maneuvering capabilities of fish of large size in the field have been described with a stereovideography system. The methodology of analysis of the three-dimensional data involved complex computation and statistical techniques beyond what had previously been performed for a two-dimensional study by Parson et al. (2011). The turning performance of the manta was

compared to that of other swimmers to evaluate the effects of large body size with a stiff body. As the body of the manta is rigid along its longitudinal axis, it was predicted that the manta would have a turning performance similar to other rigid-bodied swimmers.

MATERIALS AND METHODS

Field site and video capture

Video recordings of mantas (*Mobula birostris* Walbaum 1792) in the field were undertaken in 2008 and 2009. An evaluation of the molecular phylogeny of the genus previously called *Manta* considers that *Mobula* should be used as it has taxonomic priority (Poorvliet et al., 2015; White et al. 2017). However, the common name manta will be used throughout the manuscript as the batoid classification is currently in transition. Data collection of the maneuvering behavior of manta was performed in an open water environment around the island of Yap, Micronesia. The location has at least 65 known mantas, which frequent the lagoon inside the reef that surrounds the island (Homma et al., 1997). Mantas come inside the reef for mating activities and to visit cleaning stations (Homma et al., 1997). Video recordings of mantas was confined to a location on the north side of the island called Manta Ridge, which had access to the ocean through Mill Channel. A cleaning station was located at Manta Ridge at a depth of 24 m. Individuals were identified by the pigmentation pattern on the venter of the body (Homma et al., 1997).

To detail the kinematics of maneuvering by mantas, scaled stereo video recordings (30 frames s^{-1}) of mantas were made. With divers on SCUBA, two video cameras (Sony Handycam, model HDR-SR11; 10.2 megapixel resolution) in underwater housings (Amphibico Dive Buddy, model SR11/12) were used for video recording. Each camera was mounted on a tripod. The cameras were positioned on the bottom of the lagoon around a cleaning station approximately 5 m apart with overlapping fields of view. The two video recordings were synchronized by periodic discharges of an underwater strobe (Sea&Sea YA-40A), which was triggered by an underwater still camera (Sea&Sea Motor Marine 35, model MX-10). A three-dimensional calibration device was positioned within the center of the field of view for both cameras at a distance of approximately 6 m. The calibration device consisted of six aluminum rods (9.7 mm diameter, 0.61 m long) that were screwed into each face of a 50 mm nylon cube, providing an orthogonal arrangement of the rods. Two 38 mm diameter nylon balls were attached to each rod with one ball at the end of the rod and another positioned equidistantly on the rod at 0.3 m between the centers of the terminal ball and the central cube.

Video analysis

Video recordings were analyzed using Proanalyst Professional (Xcitex, Cambridge, MA) to manually track eight distinct points on the body in three dimensions. The eight points included right and left cephalic lobes, right and left eyes, right and left pectoral fin tips, dorsal fin tip, and base of the tail. The base of the tail coincided with the

posterior margin of the dorsal fin. The body length (L) was measured as the distance from the eye to the base of the tail. Manta body length was estimated as 1.25+0.12 m.

The digitized points through a maneuvering sequence were assigned X, Y, and Z coordinates. The pectoral fin closest to the center of a turn was referred to as the inboard fin and the fin furthest from the turn center was the outboard fin in accordance with the nomenclature of Fish and Nicastro (2003). The frequency of pectoral fin strokes was determined as the inverse of the period of at least one complete stroke cycle, where the tip of one fin could be observed. The difference in vertical displacements between the inboard and outboard fins when turning was measured when the fin tips of both fins could be observed through at least one half cycle. Maximum bank angles of the mantas executing a turn were measured from video with a protractor when the ray was oriented with the tips of the pectoral fins perpendicular to the camera view.

Principal Component Analysis

Each trajectory was tracked for intervals of 0.33 s in three-dimensions. However, one dimension was solely due to the angle of the camera and did not contribute to the turning motion of the manta ray. Because this dimension was not consistent between trajectories, the points were projected from three-dimensions into the two-dimensional turn using Principal Component Analysis (PCA). PCA is a popular approach for deriving a lower-dimensional set of features from a larger-dimensional space. This method systematically rotates the points onto new axes, each explaining less of the overall variation in the data set than the last. This process continues until all of variance has been

explained by the orthogonal components. Figure 1 shows the three-dimensional turning trajectories of four manta rays projected onto their respective first two principal components. Over 99% of the total variation in the three dimensions was explained by the first two principal components for all thirty trajectories.

Turning trajectory analysis

The trajectory of the manta was defined in rectangular principal coordinates by the plane curve $\mathbf{c}(t)=(x(t), y(t))$, where $\mathbf{c}$ is the position, t is time, and x and y are coordinates. Each of the 30 turning maneuvers were visualized as trajectories in the plane. To fully capture a turn, the turning rate (ω, deg s^{-1}), and turning radius (R, m) were estimated instantaneously every 0.33s throughout the entirety of the turn. $\omega(t)$ was defined as the derivative of the unit tangent vector to the curve, $\mathbf{T}(t)$. $R(t)$ was defined as the radius of the osculating circle, which was the best-fit circle to the curve at a given point with the same unit tangent vector and curvature. Curvature, $\kappa(t)$, was defined as the rate that the unit tangent vector changed with respect to arc length. Swimming speed (m s^{-1}) was calculated as $2\pi R \omega/360°$.

Estimates of instantaneous velocity $\mathbf{c}'(t)$ and acceleration $\mathbf{c}''(t)$ were needed to calculate ω and R. It was necessary to smooth the trajectories before estimating the required derivatives (see Smoothing Splines). ω at a point was calculated using the equation $\omega(t) = \left|\frac{d\mathbf{T}}{dt}\right| = \frac{|\mathbf{x}'(t)\mathbf{y}''(t)-\mathbf{y}'(t)\mathbf{x}''(t)|}{\mathbf{x}'(t)^2+\mathbf{y}'(t)^2}$ (in rad s^{-1}) and subsequently converted to units of deg s^{-1}. Curvature at a point was calculated using the equation $\kappa(t) = \left|\frac{d\mathbf{T}}{ds}\right| = \frac{\omega(t)}{|\mathbf{c}'(t)|}$

$$=\frac{|\mathbf{x}'(t)\mathbf{y}''(t)-\mathbf{y}'(t)\mathbf{x}''(t)|}{(\mathbf{x}'(t)^2+\mathbf{y}'(t)^2)^{3/2}}$$ (in 1 m^{-1}). Finally, the R at a point was calculated using the relation

$(t)=\frac{1}{\kappa(t)}$. The centripetal acceleration (a_c, g) was calculated as ($\mathbf{c}'^2/R$)/9.8.

The observables were time averaged to provide a single estimate of the turning rate, radius, swimming speed, and centripetal acceleration for each of the 30 turning sequences. To examine the maximal turning performance by the mantas, data were expressed as maximum and minimum values, means+one standard deviation (S.D.), median values and the means of the extreme 20% of values (i.e., minimum R, maximum ω). Choice of the extreme 20% of values was considered arbitrary but was used previously for comparisons of turning performance (Webb, 1983; Gerstner, 1999, Fish et al., 2003; Fish and Nicastro, 2003). Regression equations and correlation coefficients, r, were computed using KaleidaGraph Version 4.5 (Synergy Software, Reading, PA). Statistical significance was determined at the $P<0.5$ level.

Smoothing Splines

There were two sources of variability in the data set. The first was due to the movement of the unsteady motion of the mantas. The second was because points on the manta to be tracked on the two synchronized videos were manually tracked in the three-dimensional space. In order to get smooth trajectories of the rays from the data, smoothing splines were used in both principal component dimensions separately. Splines are a general class of piecewise polynomial functions. As is most commonly the case, cubic splines were used. This manipulation produced a continuous curve with existing first and second derivatives. Smoothing splines also have the advantage of a

regularization term that shrinks many of the estimated coefficients to zero. Instead of determining the smoothing parameter directly, the effective degrees of freedom were chosen based on the number of observed points for each ray. Based on the empirical data, the square root of the number of observations resulted in a trade-off between smooth curves and capturing local turns. The trajectories projected on to the first two principal components and the smoothed curves are displayed in Figure 1. It can be seen that this method removes fluctuations most likely due to the movement of the mantas, while also preserving the overall smooth turn of the ray.

Cross-Correlation Analysis

As two points on the body were measured for each ray every 0.33 s throughout the entire turn, the cross-correlation between the trajectories were analyzed. The cross-correlation measures the linear relationship between two time series for the shift in time between the two trajectories. The goal is to find the value of the shift that maximizes the correlation coefficient. In order to get a more stable estimate of the cross-correlation between two series, any trend and auto-correlation must be removed within the individual series. This removal is necessary because any inherent trend or auto-correlation within the individual series can artificially inflate the cross-correlation between any two series. We remove artificial inflation by using Autoregressive Moving Average (ARMA) models. These models have two parts: regressing the outcome on time shifted values (AR) and then modeling the error terms as a moving average (MA) of other error terms of time shifted values. The order (i.e., number of shifted values) for each part can be found

by examining the auto-correlation function (ACF) and partial auto-correlation function (PACF), respectively. Orders of each shifted value were chosen such that they were the largest time shift with values of ACF and PACF still significantly different from zero at the 95% level. After estimating the parameters via maximum likelihood estimation, residual values were examined between the two time series. Finally, the cross-correlation between the turning rates at both points of the body were examined.

Figure 1 illustrates an example of the data processing (i.e., PCA, Smoothing Splines, and Cross-correlation analysis) from beginning to end of a representative trajectory. Two trajectories of points on the body of a single ray were analyzed.

RESULTS

Maneuvering patterns and kinematics

Mantas were recorded singly or in pairs as they maneuvered about the cleaning station. Mantas swam 1-2 meters above the substratum. A total of seven individual mantas were recorded for 30 turning sequences. The presence of the divers and calibration device did not appear to negatively affect behavior as mantas are inquisitive (Last and Stevens, 2009). Each manta swam with an oscillatory, wing-like motion (Movie S1) as has previously been described by Klausewitz (1964) and Fish et al. (2016).

Yawing turns were accompanied with banking (rolling) of the body by 3-80° from the vertical (Fig. 2). A combination of powered (active fin strokes) and unpowered (gliding) movements was used to produce turning. Powered portions of turns were associated with asymmetrical motions of the pectoral fins. The outboard fin always

moved through a greater vertical excursion than the inboard fin by 1.7+0.6 times. The frequency of the pectoral stroke was 0.32+0.11 Hz.

The mantas swam slowly at 1.42+0.50 m s^{-1} (range: 0.46-2.51 m s^{-1}). Speed changed through the maneuver, which was associated with active fin movements interspersed with glides. Glides were executed at the end of the up-stroke. During periods of gliding, the pectoral fins were held with a dihedral orientation (Fig. 2).

Turning rates and radii

Frequency histograms for the estimated ω and R are shown in Figure 3. The data show a very skewed right distribution for both ω and R. Neither mean nor median values for ω and R were significantly correlated with swimming speed. The mean ω over 30 turning sequences was 18.26+5.90 deg s^{-1} with a median value of 10.93 deg s^{-1}. The highest measured ω was 67.32 deg s^{-1} and the mean ω for the highest 20% of values was 42.65+16.66 deg s^{-1}. The mean R over 30 turning sequences was 5.82+2.16 m with a median of 1.75 m. The smallest measured R was 0.48 m and the mean R for the smallest 20% of values was 2.05+1.26 m. The minimum length-specific radius (R/L) was 0.38 and the mean R/L for the smallest 20% of values was 1.64.

The mean and median ω decreased curvilinearly with increasing R (Fig. 4). Mean and median ω were significantly correlated with R (mean: r=0.81, P<0.05, d.f.=5; median: r=0.87, P<0.05, d.f.=5). The regression equations were:

$$\text{Mean } \omega = 51.58\, R^{-0.74}$$

$$\text{Median } \omega = 17.1 \ R^{-0.62}$$

The centripetal acceleration (a_c) was low, ranging from 0.01 to 0.18 g for mean values and 0.00 to 0.03 g for median values. a_c increased linearly with ω (Fig. 5), where the regression of the mean values was significantly correlated ($r=0.76$, $P<0.025$, d.f.=5), but the median values were not significantly correlated ($r=0.61$, ns, d.f.=5). The regression equations were:

$$\text{Mean } a_c = 0.009 + 0.002 \ \omega$$

$$\text{Median } a_c = 0.004 + 0.0003 \ \omega$$

Of the 30 turns recorded, 17 sequences had enough overlap between two points on the body to perform a cross-correlation analysis. Of those 17, ten had a cross-correlation value that was only significantly different from zero at a time shift of zero (i.e., the two series had a strong linear relationship at the exact same time). The remaining seven sequences only included one that had a cross-correlation that was significantly different from zero at a time shift within a reasonable amount of time (2 s). Indeed, one sequence resulted in a significant cross-correlation when the tailbase lagged the left cephalic lobe by 0.66 s. The other significant time shifts occurred after more than 2 s and were very infrequent. These types of time shifts suggest that they were spurious associations between two points on a large body. The fact that there were mainly significant cross-

correlations between ω at a time shift of zero implies that the two points on the body were effectively turning at the same rate. This was expected for a rigid-bodied animal.

DISCUSSION

Stereovideography advantages and limitations

The maneuvering performance of the manta was assessed by the use of stereovideography in the field. This was the first such analysis of a large aquatic animal in its natural surroundings. As opposed to the laboratory studies and the use of tags in the field, stereovideography has three distinct advantages (Boisclair, 1992). First analysis employing stereovideography allows a detailed qualitative and quantitative assessment of movement. The body orientation and movement of fins can be directly observed to determine their influence on maneuverability and agility. When appropriately scaled, speed can be measured and changes in speed can be associated with distinct fin movements. The second advantage is that this procedure allows measurement of the animal's movement in three dimensions. As fish are capable of swimming and maneuvering in three dimensions, the method can capture movements in their natural habitats. This was advantageous for examination of manta due to its size and operation in a large volume space. Lastly, in contrast to the attachment of tags on large aquatic animals, stereovideography can be used without influencing behavior, increasing drag and thus swimming performance, and injuring the animal (Read and Westgate, 1997; Watson and Granger, 1998; Chilvers et al., 2001; Pavlov et al., 2007; Dewar et al., 2008; Balmer et al., 2010; Jones et al., 2011).

Despite the advantages, there are also limitations to the use of stereovideography in the field. Boisclair (1992) considered that visibility was the most serious limitation in video recording underwater, which would be associated with low light intensity due to turbidity, time of day, and depth. Regarding the swimming by the manta in this study, visibility affected the distance from the cameras that movements of manta could be recorded. In addition, the low light levels made it difficult to manually track the distinct points on the animal. This reduction in accuracy potentially added to the error in digitizing the trajectory of a maneuver by the manta. Therefore, mathematical analysis was required to statistically determine the swimming path of the manta. Another limitation was that video recording was confined to spatially limited locations where mantas were known to frequent, but may not have displayed maximal maneuvering performance. As a result, the data were highly skewed. Mantas swimming and foraging in the open ocean may have different degrees of maneuvering performance compared to movement around reef locations.

Another logistical limitation to stereovideography in the field was related to maintaining a fixed frame of reference. Cameras were positioned on tripods that were placed on the bottom. The rigid positioning of the cameras constrained what videos could be used and were dependent on the behavior of the animal to predictably perform in the chosen location. Stereovideography could not be performed in the mid-water column in the field due to independent movements by the divers and independent movements by the mantas with a background with no fixed markers.

Manta turning performance

As displayed from videos of mantas in areas around the cleaning stations, these pelagic fish demonstrated maneuverability and agility that would have been considered uncharacteristic of such large animals. Mantas generally swim slow around cleaning stations and will hover above the bottom to be cleaned by wrasse *(Labroides dimidiatus)* or small shrimp (Homma et al., 1997). The speeds that were used to perform the turns ($1.42+0.50$ m s^{-1}) were higher than swimming speeds reported for mantas while foraging (range 0.25-0.47 m s^{-1}) and migrating (0.97 m s^{-1}) when measured from satellite tags (Graham et al, 2012; Jaine et al., 2014). The low speeds from satellite tags may be due to the intermittent uploading of positional data that does not take into account maneuvers and changing depth. However, Yano et al. (1999) reported that mantas can swim at 2.78-4.17 m s^{-1} when males are chasing females during mating. In addition, mantas perform aerial leaps clearing the water (Coles, 1916; Rayner, 1986; Homma et al., 1997; Duffy and Abbott, 2003; De Boer et al., 2015). The physics of such leaps requires high-speed swimming (Rohr et al., 2002). By conservation of energy, a 2,722 kg manta leaping 1 m into the air would require an initial speed of 4.43 m s^{-1}, which is 3.1 times the mean speed for mantas performing turning maneuvers in this study.

The turns performed by mantas were produced by a combination of translational and rotational movements. As mantas have a rigid body, the turning performance measured from anterior and posterior points on the body were the same and thus reflect the turning performance of the center of mass (COM). The center of mass would be on a

line between the two points of measurement. For mantas as well as other mobuliform rays, the COM is located at 47% of body length (Fontanella et al., 2013).

The mantas were able to execute turns by unpowered glides and powered flapping motions. Unpowered glides have been observed in myliobatid rays that swim with an oscillatory, lift-based propulsion (Rosenberger, 2001; Parson et al., 2011). Gliding turns were also noted for other oscillatory, lift-based swimmers including penguins, cetaceans, and sea lions (Hui, 1985, Fish, 2002; Fish *et al*., 2003). In powered turns by the manta and other myliobatid rays, propulsive motions of the pectoral fins were evident throughout the entire turn (Parson et al., 2011; this study). Turning was accomplished by differential movements of the pectoral fins with the outboard fin flapping at a higher frequency than the inboard fin.

Unpowered turns would rely on banking. Banking was required to generate the centripetal force to produce a curved trajectory. Banking is a rolling maneuver that provides a greater projected area facing the axis of the turn (Fish *et al*., 2003, 2012; Parson et al., 2011). Lift is generated primarily from the pectoral fins and additionally from the cambered body (Parson et al., 2011; Fish *et al*., 2012, 2016). The lift vector is perpendicular to the frontal plane of the body and fins of the ray (Fig. 6). The lift opposes a hydrodynamic force generated from the combined forces of the drag on the body and fins in the transverse plane and weight of the negatively buoyant animal. When banking through the turn, the lift vector is canted at an angle, which is directed toward the inside of the turn (Fish et al., 2012). The horizontal component of the lift vector generated by the pectoral fins produces a centripetal force, which turns the manta. Banking is a more economical means of moving in a circular path than generating an asymmetric thrust

(Weihs, 1981). Another myliobatid ray, cownose ray (*Rhinoptera bonasus*), banks by 65° and 70° in yawing turns (Parson et al., 2011). High bank angles are characteristic of aquatic animals that lack median fins and turn using elongate paired fins (Fish and Battle, 1995; Fish, 2002; Fish et al., 2003, 2012).

The wide variation for *R* was due to the movements of the mantas within a large volume. The turns may not represent the minimum *R* that could potentially be accomplished. Small *R* appeared to be associated with slow swimming speeds. The mean *R* for the smallest 20% of values was 2.05+1.26 m performed at a swimming speed of 1.06+0.39 m s^{-1}, whereas the mean *R* for the largest 20% of values was 9.31+1.73 m with a mean swimming speed of 1.46+0.57 m s^{-1}. Indeed, the minimum *R* of 0.48 m for a manta occurred at the slowest recorded swimming speed of 0.45 m s^{-1}. Fish and Nicastro (2003) reported that turning radius was directly but weakly related to swimming speed in whirligig beetles (*Dineutes horni*).

The highest turning rates (ω) for mantas were similar to the performance of cownose rays. Parson et al. (2011) found that cownose rays performed yawing turns at a rate of 44.4 deg s^{-1} (Parson et al., 2011). This value of ω was only 1.04 times greater than the value for the mantas despite the extreme size difference.

Aside from yawing turns, mantas are able to turn by pitching to execute somersaults in a looping circular trajectory (Coles, 1916; Clark, 1969; Duffy and Abbott, 2003; Fish et al., 2012). This somersault maneuver is used by mantas for feeding on concentrations of krill (Bigelow and Schroeder, 1953; Homma et al., 1999; Duffy and Abbott, 2003). Fish et al. (2012) video recorded somersaulting of a manta in an aquarium and measured the ray's turning performance for a single maneuver. *R/L* of the loop was

approximately 0.7. The ω of the maneuver was 41.5 deg s^{-1} (Fish et al., 2012). This turning performance was greater than yawing turns for *R/L* by 1.7 times, but approximated the mean ω for the highest 20% of yawing turns for mantas measured in this study.

The difference in performance for *R/L* represents limitations due to flexibility of the pectoral fins versus the body that differentially affect movement about the rotation axes (pitch, yaw, roll). In yawing turns, torques can be generated from both passive and active synchronization and movements of the fins in addition to a centripetal force from banking. For pitching turns, the body is rigid in the sagittal plane resisting pitch (Fontanella et al., 2013). However by simultaneous movements and chordwise bending of the flexible pectoral fins, mantas can execute small radius turns in the sagittal plane. This action was demonstrated in a YouTube video entitled, "Book'em Danno: Klepto Manta Mugs Cameraman" (https://www.youtube.com/watch?v=I5wY38dhFPA) at 0:24 s displayed at normal speed and at 0:32 s in slow motion. In this case, the manta was estimated to make an 180º turn at 104 deg s^{-1}.

Comparative turning performance

The ability to maneuver is a fundamental locomotor behavior. Maneuvering has been studied for a number of aquatic animals in both the laboratory and field. In general, the size of turning radii is largely dependent on body size. Small animals can perform smaller radius turns than large animals (Howland, 1974; Fish and Nicastro, 2003). However when the turn radius is scaled to body length, this generality does not always hold. Circular turns by small fish typically have radii of less than 0.2 *L* (Webb, 1983;

Domenici and Blake, 1997; Gerstner, 1999). The 12.4 mm whirligig beetle (*Dineutes horni*) displayed a minimum turn radius of 0.24 *L* (Fish and Nicastro, 2003), whereas the minimum turn radius was 0.09 *L* for a sea lion (*Zalophus californianus*) of 1.89 m in length (Fish et al., 2003) and 0.11 *L* for 5.1 m killer whale (*Orcinus orca*) (Fish, 2002). In comparison, mantas displayed relatively large length-specific turn radius of 0.37 *L*.

The limited maneuverability of the manta may have been due in part to motivation by the animal. As the mantas were freely swimming in an unconstrained environment, there was no incentive to make the tightest turn possible. Experiments performed on fish stimulated to yield fast-starts demonstrated that fish could turn with radii down to 0.06 *L* (Domenici and Blake, 1997). In addition, the mantas are filter feeders and do not have to elicit small radius turns to acquire their planktonic food. The radius of the pitching somersault maneuver used by feeding mantas was 70% greater than the minimum yawing turn radius for the mantas observed around Yap. (Fish et al., 2012).

Another constraint on turning performance was the relatively inflexible body of the manta. The large proportion of the body devoted to the branchial apparatus and the extended base of the thick pectoral fins limit flexibility in both the sagittal and frontal planes. The turn rate, ω, for mantas was lower than for similarly sized flexible-bodies swimmers (Fig. 7). Similarly, a_c for the manta was lower than for flexible-bodied animals (Fish and Nicastro, 2003). This assertion was largely a consequence of the wide turn radius and slow swimming speed for the manta compared to flexible-bodied animals.

Fish and Nicastro (2003) compared the ω of flexible- and rigid-bodied animals of different body sizes. When a line was drawn on a logarithmic scale between the maximum ω for the smallest (whirligig beetle: 4437.5 deg s^{-1}) and largest submarine

(USS Albacore: 3 deg s^{-1}) rigid bodies, flexible-bodied animals (e.g., fish, dolphins, sea lions) were positioned above the line and rigid-bodied animals (i.e., boxfish, squid, turtle, rays) were positioned below the line (Fish and Nicastro, 2003; Rivera et al., 2006; Parson et al., 2011). It was shown that for equivalent body sizes, flexible-bodied swimmers had higher turning rates than rigid-bodied animals. The humpback whale (*Megaptera novaeangliae*) is a flexible-bodied filter feeder with highly mobile flippers that has high agility for its size (Edel and Winn, 1978). Using tags with 3-axis magnetometer and accelerometers on humpback whales, Wiley et al. (2011) determined that a whale feeding on schools of small fish with an upward-spiral bubble-net feeding behavior had a maximum turn rate of 13.8 deg s^{-1}. Assuming a mature humpback whale of 12 m in length (Winn and Reichley, 1985), the turn rate of the whale was 11% higher than for an equivalent sized rigid-bodied swimmer.

Mantas have a low ω compared to the various flexible-bodied animals (Fig. 7). The relatively rigid body, particularly with to lateral bending, would limit yawing turns. In this regard, the position of mantas below the line for rigid-bodied swimmers was consistent with previous studies (Fig. 7; Fish and Nicastro, 2003; Rivera et al., 2006; Parson et al., 2011). However, mantas can compensate for their inflexibility by using the flexible distal portions of the pectoral fins or asymmetrical fin movements, and banking maneuvers (Fish et al., 2012, 2016; Russo et al., 2015). As a result, ω for mantas is only 22.7% lower than the predicted ω for an equivalent rigid-bodied swimmer. In addition to ω of the manta located closer to the line separating rigid-bodied from flexible-bodied than other batoids, the maximum ω of manta was 40.3% and 110.4% greater than oscillatory-swimming and undulatory-swimming rays, respectively (Parson et al., 2011).

Walker (2000) insisted that ω for rigid-bodied swimmers was at least six to eight times lower than predicted for flexible-bodied animals.

Conclusions

The analysis of the three-dimensional turning performance of animals in the field presents a number of challenges. The use of stereovideography has advantages that permit the ability to determine movements in a three-dimensional space with the associated body movements. Using this technique, maneuverability and agility of manta rays were analyzed in their natural habitat. Mantas were shown to bank and make small radius turns with turn rates as high as 67.32 deg s^{-1}. The data support the general conclusion that the rigid body of manta rays limits turning performance compared to flexible-bodied animals. In addition, the flexibility in the pectoral displayed by the manta allowed these large rays to perform turning maneuvers at a higher rate than other batoid rays. Such limitations are important as attempts are made to produce aquatic bio-robots inspired by the morphology and swimming kinematics of rays (Moored et al., 2011; Fish et al., 2016, 2016; Park et al., 2016).

manager) and the Office of Naval Research for funding of the project (N000140810642).

The research was approved by the West Chester University Institutional Animal Care and

Use Committee (Fish 08-01). Data are available in the institutional data repository

(http://digitalcommons.wcupa.edu/bio_data/).

References

Balmer, B. C., Schwacke, L. H., and Wells, R. S. (2010). Linking dive behavior to satellite-linked tag condition for a bottlenose dolphin (*Tursiops truncatus*) along Florida's northern Gulf of Mexico coast. *Aquat. Mamm*, **36,** 1-8.

Bigelow, H. B. and Schroeder, W. C. (1953). *Fishes of the Western North Atlantic. Part 2. (Sawfishes, Guitarfishes, Skates, Rays and Chimaeroides).* Sears Foundation for Marine Research, Yale University.

Blake, R. W., Chatters, L. M., and Domenici, P. (1995). The turning radius of yellowfin tuna (*Thunnus albacores*) in unsteady swimming manoeuvres. *J. Fish Biol.* **46,** 536-538.

Blevins, E. L. and Lauder, G. V. (2012). Rajiform locomotion: three-dimensional kinematics of the pectoral fin surface during swimming in the freshwater stingray *Potamotrygon orbignyi*. *J. Exp. Biol.* **215**, 3231-3241.

Boisclair, D. (1992). An evaluation of the stereocinematographic method to estimate fish swimming speed. *Can. J. Fish. Aquat. Sci*. **49**, 523-531.

Cheneval, O., Blake, R. W., Trites, A. W. and Chan, K. H. S. (2007). Turning maneuvers in Steller sea lions (*Eumatopias jubatus*). *Mar. Mamm. Sci*. **23**, 94-109.

Chilvers, B. L., Corkeron, P. J., Glnashard, W. H., Long, T. R., and Martin, A. R. (2001). A new VHF tag and attachment technique for small cetaceans. *Aquat. Mamm.* **27**, 11-15.

Clark, E. (1969). *Lady with a Spear*. New York: Harper and Row.

Coles, R. J., 1916. Natural history notes on the devilfish, *Manta birostris* (Walbaum) and

    Mobula olfersi (Müller). *Bull. Am. Mus. Nat. Hist*. **35**, 649-657.

Compagno, L. J. V. (1999). Systematics and body form. In *Sharks, Skates, and Rays: The*

    Biology of Elasmobranch Fishes (ed. W. C. Hamlett), pp. 1-42. Baltimore, MD:

    Johns Hopkins University Press.

Danos, N. and Lauder, G. V. (2007). The ontogeny of fin function during routine turns in

    zebrafish *Danio rerio*. *J. Exp. Biol.* **210**, 3374-3386.

Deacon K.; Last P.; McCosker, J.E.; Taylor, L.; Tricas, T.C.; Walker, T.I. (1997). *Sharks*

    and Rays. San Francisco, CA: Fog City Press.

De Boer, M. N., Saulino, J. T., Lewis, T. P. and Notarbartolo-Di-Sciara, G. (2015). New

    records of whale shark (*Rhincodon typus*), giant manta ray (*Manta birostris*) and

    Chilean devil ray (*Mobula tarapacana*) for Suriname. *Mar. Biodivers Rec.* **8**, 1-8.

Dewar, H., Mous, P., Domeier, M., Muljadi, A., Pet, J., and Whitty, J. (2008).

    Movements and site fidelity of the giant manta ray, *Manta birostris*, in the

    Komodo Marine Park, Indonesia. *Mar. Biol.* **155**, 121-133.

Domenici, P, and Blake, R. W. (1991). The kinematics and performance of the escape

    response in the angelfish (*Pterophyllum eimekei*). *J. Exp. Biol.* **156**, 187-205.

Domenici, P. and Blake, R. W. (1997). The kinematics and performance of fish fast-start

    swimming. *J. Exp. Biol.* **200**, 1165-1178.

Domenici, P., Standen, E. M., and Levine, R. P. (2004). Escape manoeuvres in the spiny

    dogfish (*Squalus acanthias*). *J. Exp. Biol.* **207,** 2339-2349.

Duffy, C. A. J. and Abbott, D. (2003). Sightings of mobulid rays from northern New Zealand, with confirmation of the occurrence of *Manta birostris* in New Zealand waters. *NZ J. Mar. Freshw. Res*. **37**, 715-721.

Edel, R. K. and Winn, H. E. (1978). Observations on underwater locomotion and flipper movement of the humpback whale *Megaptera novaeangliae*. *Mar. Biol.* **48**, 279-287.

Fish, F. E. (1997). Biological designs for enhanced maneuverability: analysis of marine mammal performance In *Proceedings of the Tenth International Symposium on Unmanned Untethered Submersible Technology,* pp. 109-117. Durham, New Hampshire: Autonomous Undersea Systems Institute.

Fish, F. E. (2002). Balancing requirements for stability and maneuverability in cetaceans. *Integ. Comp. Biol.* **42**, 85-93.

Fish, F. E. and Battle, J. M. (1995). Hydrodynamic design of the humpback whale flipper. *Journal of Morphology* **225**, 51-60.

Fish, F. E., Hurley, J., and Costa, D. P. (2003). Maneuverability by the sea lion, *Zalophus californianus*: Turning performance of an unstable body design. *J. Exp. Biol.* **206**, 667-674.

Fish, F. E. and Nicastro, A. J. (2003). Aquatic turning performance by the whirligig beetle: constraints on maneuverability by a rigid biological system. *J. Exp. Biol.* **206**, 1649-1656.

Fish, F. E., Bostic, S. A., Nicastro, A. J. and Beneski, J. T. (2003). Death roll of the alligator: mechanics of twist feeding in water. *J. Exp. Biol.* **210**, 2811-2818.

Fish, F. E., Haj-Hariri, H., Smits, A. J., Bart-Smith, H., and Iwasaki, T. (2012). Biomimetic swimmer inspired by the manta ray. In *Biomimetics: Nature-Based Innovation* (ed. Y. Bar-Cohen), pp. 495-523. Boca Rotan, FL: CRC Press.

Fish, F. E. and Domenici, P. (2015). Introduction to the symposium-Unsteady aquatic locomotion with respect to eco-design and mechanics. *Integ. Comp. Biol.* **55**, icv039

Fish, F. E. and Hoffman, J. L. (2015). Stability design and response to waves by batoids. *Integ. Comp. Biol.* **55**, 648-661.

Fish, F. E., Schreiber, C. M., Moored, K. M., Liu, G., Dong, H. and Bart-Smith, H. (2016). Hydrodynamic performance of aquatic flapping: Efficiency of underwater flight in the manta. *Aerospace* **3**, 20.

Fontanella, J. E., Fish, F. E., Barchi, E. I., Campbell-Malone, R., Nichols, R. H., DiNenno, N. K., and Beneski, J. T. (2013). Two- and three-dimensional geometries of batoids in relation to locomotor mode. *J. Exp. Mar. Biol. Ecol.* **446**, 273-281.

Foyle, T. P. and O'Dor, R. K. (1988). Predatory strategies of squid (*Illex illecebrosus*) attacking large and small fish. *Mar. Behav. Physiol.* **13**, 155-168.

Frey E. and Salisbury, S.W. (2001). The kinematics of aquatic locomotion in *Osteolaemus tetraspis* Cope. In *Crocodilian Biology and Evolution* (ed. G. C. Grigg, F. Seebacher and C. E. Franklin), pp. 165-179. Chipping Norton, Australia: Surrey Beatty.

Gerstner, C. L. (1999). Maneuverability of four species of coral-reef fish that differ in body and pectoral-fin morphology. *Can. J. Zool.* **77**, 1102-1110.

Geurten, B. R., Niesterok, B., Dehnhardt, G. and Hanke, F. D. (2017). Saccadic

movement strategy in a semiaquatic species–the harbour seal (*Phoca vitulina*). *J.*

Exp. Biol. **220**, 1503-1508.

Goldbogen, J. A., Calambokidis, J., Friedlaender, A. S., Francis, J., DeRuiter, S. L.,

Stimpert, A. K., Falcone, E., and Southall, B. L. (2013). Underwater acrobatics by

the world's largest predator: 360° rolling manoeuvres by lunge-feeding blue

whales. *Biol. Lett.* **9**, 20120986.

Graham, R. T., Witt, M. J., Castellanos, D. W., Remolina, F., Maxwell, S., Godley, B. J.

and Hawkes, L. A. (2012). Satellite tracking of manta rays highlights challenges

to their conservation. *PLos One* **7**, e36834.

Hazen, E. L., Friedlaender, A. S., Thompson, M. A., Ware, C. R., Weinrich, M. T.,

Halpin, P. N., and Wiley, D. N. (2009). Fine-scale prey aggregations and foraging

ecology of humpback whales *Megaptera novaeangliae*. *Mar. Ecol. Prog. Ser.*

395, 75-89.

Helmer, D., Geurten, B. R., Dehnhardt, G., and Hanke, F. D. (2016). Saccadic movement

strategy in common cuttlefish (*Sepia officinalis*). *Front. Physiol.* **7**, 660.

Homma, K., Maruyama, T., Itoh, T., Ishihara, H., and Uchida, S. (1997). Biology of the

manta ray, *Manta birostris* Walbaum, in the Indo-Pacific. *Indo-Pacific Fish Biol.:*

Proc. 5th Int. Conf. Indo-Pacific Fishes, Noumea, 209-216.

Howland, H. C. (1974). Optimal strategies for predator avoidance: The relative

importance of speed and manoeuvrability. *J. Theor. Biol.* **47**, 333-350.

Hughes, N. F., and Kelly, L. H. (1996). New techniques for 3-D video tracking of fish swimming movements in still or flowing water. *Can. J. Fish. Aqu. Sci.* **53**, 2473-2483.

Hughes, N. F., Hayes, J. W., Shearer, K. A. and Young, R. G. (2003). Testing a model of drift-feeding using three-dimensional videography of wild brown trout, *Salmo trutta*, in a New Zealand river. *Can. J. Fish. Aqu. Sci.* **60**, 1462-1476.

Hui, C. A. (1985). Maneuverability of the Humboldt penguin (*Spheniscus humboldti*) during swimming. *Can. J. Zool*. **63,** 2165-2167.

Jaine, F.R.A., Rohner, C.A., Weeks, S.J., Couturier, L.I.E., Bennett, M.B., Townsend, K.A. and Richardson, A.J. (2014). Movements and habitat use of reef manta rays off eastern Australia: offshore excursions, deep diving and eddy affinity revealed by satellite telemetry. *Mar. Ecol. Progr. Ser.* **510**, 73-86.

Jastrebsky, R. A., Bartol, I. K., and Krueger, P. S. (2016). Turning performance in squid and cuttlefish: unique dual-mode, muscular hydrostatic systems. *J. Exp. Biol.* **219**, 1317-1326.

Jastrebsky, R. A., Bartol, I. K., and Krueger, P. S. (2017). Turning performance of brief squid *Lolliguncula brevis* during attacks on shrimp and fish. *J. Exp. Biol*. **220**, 908-919.

Jones, T. T., Bostrom, B., Carey, M., Imlach, B., Mikkelsen, J., Ostafichuk, P., Eckert, S., Opay, P. Swimmer, Y., Seminoff, J. A., and Jones, D. R. (2011). Determining transmitter drag and best-practice attachment procedures for sea turtle biotelemetry. *NOAA Tech Memo NMFS-SWFSC*, **480**, 58.

Kajiura, S. M., Forni, J. B., and Summers, A. P. (2003). Maneuvering in juvenile carcharhinid and sphyrnid sharks: the role of the hammerhead shark cephalofoil. *Zoology* **106**, 19-28.

Kitchen-Wheeler, Anne-Marie. (2010). Visual identification of individual manta ray (*Manta alfredi*) in the Maldives Islands, Western Indian Ocean. *Mar. Biol. Res.* **6**, 351-363.

Klausewitz, W. (1964). Der Lokomotionsmodus der Flügelrochen (Myliobtoidei). *Zool. Anz.* **173**, 110-120.

Last, P. R. and Stevens, J. D. (2009). *Sharks and Rays of Australia*. Cambridge, MA: Harvard University Press.

Maresh, J. L., Fish, F. E., Nowacek, D. P., Nowacek, S. M. and Wells, R. S. (2004). High performance turning capabilities during foraging by bottlenose dolphins. *Mar. Mamm. Sci.* **20,** 498-509.

Marshall, A. D., Compagno, L. J. V., and Bennett, M. B. (2009). Redescription of the genus Manta with resurrection of *Manta alfredi* (Krefft, 1868)(Chondrichthyes; Myliobatoidei; Mobulidae). *Zootaxa* **2301**, 1-28.

Miller, D. (1991). *Submarines of the World*. New York: Orion Books.

Moored, K. W., Fish, F. E., Kemp, T. H. and Bart-Smith, H. (2011). Batoid fishes: inspiration for the next generation of underwater robots. *Mar. Tech. Soc. J.* **45**, 99-109.

Norberg, U. and Rayner, J. M. V. (1987). Ecological morphology and flight in bats (Mammalia: Chiroptera): wing adaptations, flight performance, foraging strategy and echolocation. *Phil. Trans. Roy. Soc*. B **316**, 335-427.

Parson, J., Fish, F. E., and Nicastro, A. J. (2011). Turning performance in batoid rays: Limitations of a rigid body. *J. Exp. Mar. Biol. Ecol.* **402**, 12-18.

Park, S.J., Gazzola, M., Park, K.S., Park, S., Di Santo, V., Blevins, E.L., Lind, J.U., Campbell, P.H., Dauth, S., Capulli, A.K., Pasqualini, F.S., Ahn, S., Cho, A., Yuan, H., Maoz, B. M., Vijaykumar, R., Choi, J-W., Diesseroth, K., Lauder, G. V., Mahadevan, L. and Parker, K. K. (2016). Phototactic guidance of a tissue-engineered soft-robotic ray. *Science* **353**, 158-162.

Pavlov, V. V., Wilson, R. P., and Lucke, K. (2007). A new approach to tag design in dolphin telemetry: Computer simulations to minimise deleterious effects. *Deep Sea Res. Pt. II* **54**, 404-414.

Perlmutter, A. (1961). *Guide to Marine Fishes*. New York University Press: New York.

Poortvliet, M., Olsen, J.L., Croll, D.A., Bernardi, G., Newton, K., Kollias, S., O'Sullivan, J., Fernando, D., Stevens, G., Magaña, F.G., Seret, B., Wintner, S. & Horau, G. 2015. A dated molecular phylogeny of manta and devil rays (Mobulidae) based on mitogenome and nuclear sequences. *Mol. Phylogenet. Evol*. **83**,72-85.

Rayner, J. M. (1986). Pleuston: animals which move in water and air. *Endeavour* **10,** 58-64.

Read, A. J. and Westgate, A. J. (1997). Monitoring the movements of harbor porpoises (*Phocoena phocoena*) with satellite telemetry. *Mar. Biol*. **130**, 315-322.

Rivera, G., Rivera, A. R. V., Dougherty, E. E., and Blob, R. W. (2006). Aquatic turning performance of painted turtles (*Chrysemys picta*) and functional consequences of a rigid body design. *J. Exp. Biol.* **209**, 4203-4213.

Rohr, J. J., Fish, F. E., and Gilpatrick, J. W. 2002. Maximum swim speeds of captive and free ranging delphinids: critical analysis of extraordinary performance. *Mar. Mamm. Sci.* **18**, 1-19.

Rosenberger, L. J. (2001). Pectoral fin locomotion in batoid fishes: undulation *versus* oscillation. *J. Exp. Biol.* **204**, 397-394.

Russo, R. S., Blemker, S. S., Fish, F. E. and Bart-Smith, H. (2015). Biomechanical model of batoid skeletal structure and kinematics: implications of bio-inspired design. *Bioinspir. Biomim.* **10**, 46002.

Schrank, A.J., Webb, P.W. and Mayberry, S. (1999). How do body and paired-fin positions affect the ability of three teleost fishes to maneuver around bends? *Can. J. Zool.* **77**, 203-210.

Tytell, E.D., Standen, E.M. and Lauder, G.V. (2008). Escaping flatland: Three-dimensional kinematics and hydrodynamics of median fins in fishes. *J. Exp. Biol.* **211**, 187-195.

Walker, J. A. (2000). Does a rigid body limit maneuverability? *J. Exp. Biol.* **203**, 3391-3396.

Walker, J. A. (2004). Kinematics and performance of maneuvering control surfaces in teleosts fishes. *IEEE J. Ocean. Eng.* **29**, 572-584.

Ware, C., Friedlaender, A. S. and Nowacek, D. P. (2011). Shallow and deep lunge feeding of humpback whales in fjords of the West Antarctic Peninsula. *Mar. Mamm. Sci.* **27**, 587-605.

Ware, C., David N. Wiley, Ari S. Friedlaender, Mason Weinrich, Elliott L. Hazen, Alessandro Bocconcelli, Susan E. Parks, Alison K. Stimpert, Mike A. Thompson,

and Kyler Abernathy. 2014. Bottom side‐roll feeding by humpback whales (*Megaptera novaeangliae*) in the southern Gulf of Maine, USA. *Mar. Mamm. Sci.* **30**, 494-511.

Watson, K. P., and Granger, R. A. (1998). Hydrodynamic effect of a satellite transmitter on a juvenile green turtle (*Chelonia mydas*). *J. Exp. Biol*., **201**, 2497-2505.

Webb, P. W. (1976). The effect of size on the fast-start performance of rainbow trout. *Salmo gairdneri*, and a consideration of piscivorous predator-prey interactions. *J. Exp. Biol.* **65,** 157-177.

Webb, P. W. (1978) Fast-start performance and body form in seven species of teleosts fish. *J. Exp. Biol.* **74,** 211-226.

Webb, P. W. (1983). Speed, acceleration and manoeuverability of two teleost fishes. *J. Exp. Biol.* **102,** 115-122.

Webb, P. W. (1994). The biology of fish swimming. In *Mechanics and Physiology of Animal Swimming* (eds. L. Maddock, Q. Bone, and J. M. V. Rayner), pp. 45-62. Cambridge, UK: Cambridge University Press.

Webb, P. W. 1997. Designs for stability and maneuverability in aquatic vertebrates: What can we learn? In: Tenth International Symposium on Unmanned Untethered Submersible Technology: Proceedings of the Special Session on Bio-Engineering Research Related to Autonomous Underwater Vehicles, pp. 86-108. Autonomous Undersea System Institute, Durham, New Hampshire.

Webb, P. W. (2006) Stability and maneuverability. In *Fish Biomechanics* (eds. R. E. Shadwick and G. V. Lauder), pp. 281-332. San Diego: Academic Press.

Webb, P. W. and Keyes, R. S. (1981). Division of labor between median fins in swimming dolphin fish. *Copeia* **1981,** 901-904.

Webb, P. W., LaLierte, G. D. and Schrank, A. J. (1996). Does body and fin form affect the maneuverability of fish traversing vertical and horizontal slits. *Environ. Biol. Fish.* **46**, 7-14.

Webb, P. W. and Fairchild, A. G. (2001). Performance and maneuverability of three species of teleostean fishes. *Canadian Journal of Zool*ogy **79,**1866-1877.

Weihs, D. (1981). Effects of swimming path curvature on the energetics of fish motion. *Fisheries Bulletin* **79,** 171-176.

Weihs, D. and Webb, P. W. (1984). Optimal avoidance and evasion tactics in predator-prey interactions. *J Theor. Biol.* **106,** 189-206.

Wiley, D., Ware, C., Bocconcelli, A., Cholewiak, D., Friedlaender, A., Thompson, M. and Weinrich, M. (2011). Underwater components of humpback whale bubble-net feeding behaviour. *Behaviour* **148**, 575-602.

Williams, T. M., Fuiman, L. A. and Davis, R. W. 2015. Locomotion and the cost of hunting in large, stealth marine carnivores. *Integ. Comp. Biol*. **55**, 673-682.

Williams, W. T., Corrigan, S., Yang, L., Henderson, A. C., Bazinet, A. L., Swofford, D. L. and Naylor, G. J. P. (2017). Phylogeny of the manta and devilrays (Chondrichthyes: Mobulidae), with an updated taxonomic arrangement for the family. *Zool. J. Linn. Soc*. **20**, 1-26.

Winn, H. E. and Reichley, N. E. (1985). Humpback whale *Megaptera novaeangliae* (Borowski, 1781). In *Handbook of Marine Mammals*, Vol. 3: *The Sirenians and*

Baleen Whales (eds. S. H. Ridgway, and R. Harrison), pp. 241-273. London: Academic Press.

Yano, K., Sato, F. and Takahashi, T. (1999). Observations of mating behavior of the manta ray, *Manta birostris*, at the Ogasawara Islands. *Ichthyol. Res*. **46**, 289–296.
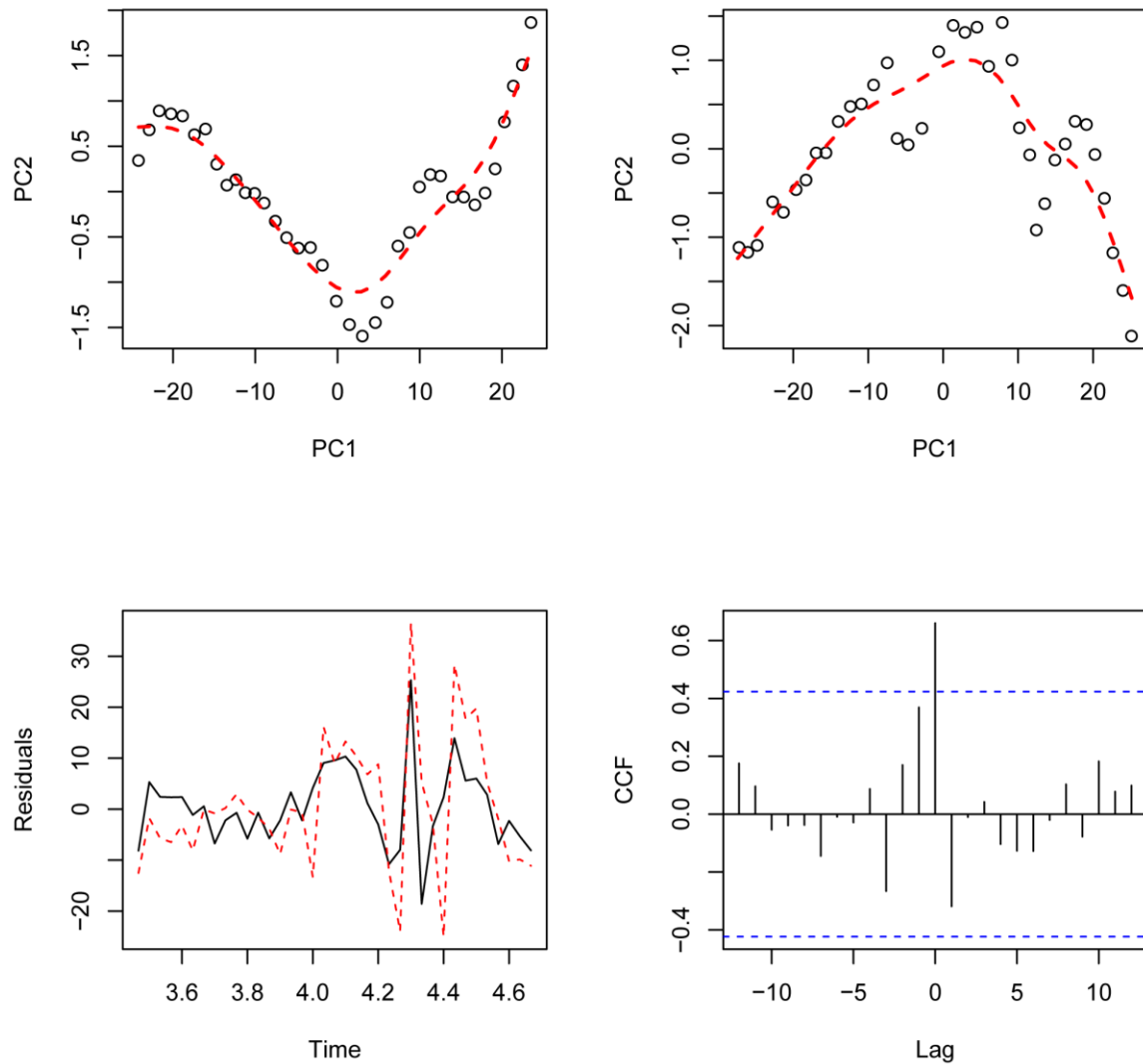
Figures

Figure 1. The plots in the top left and top right panels are the projections of trajectories into the first two principal component space. Smoothing splines were then used to remove some of the variation. The smooth, continuous curve for each point on the body is shown in the dashed, red line. The bottom left panel displays residual values of the

estimated ω after applying the appropriate ARMA model to each time series. The solid

black lines are for the dorsal point and the dashed red lines are for the cephalic lobe point.

Finally, the plot in the bottom right panel shows the cross-correlation coefficient between

the two time series at various time shifts. Any bar that exceeds the dashed blue lines is

considered to have a cross-correlation significantly different from 0 for that particular

time shift.

Figure 2. Still images from video of mantas during turning maneuvers around the three-dimensional calibration device, which is shown behind the manta. The manta is shown banking under active propulsion (left) and while gliding with the pectoral fins held with a positive dihedral (right).
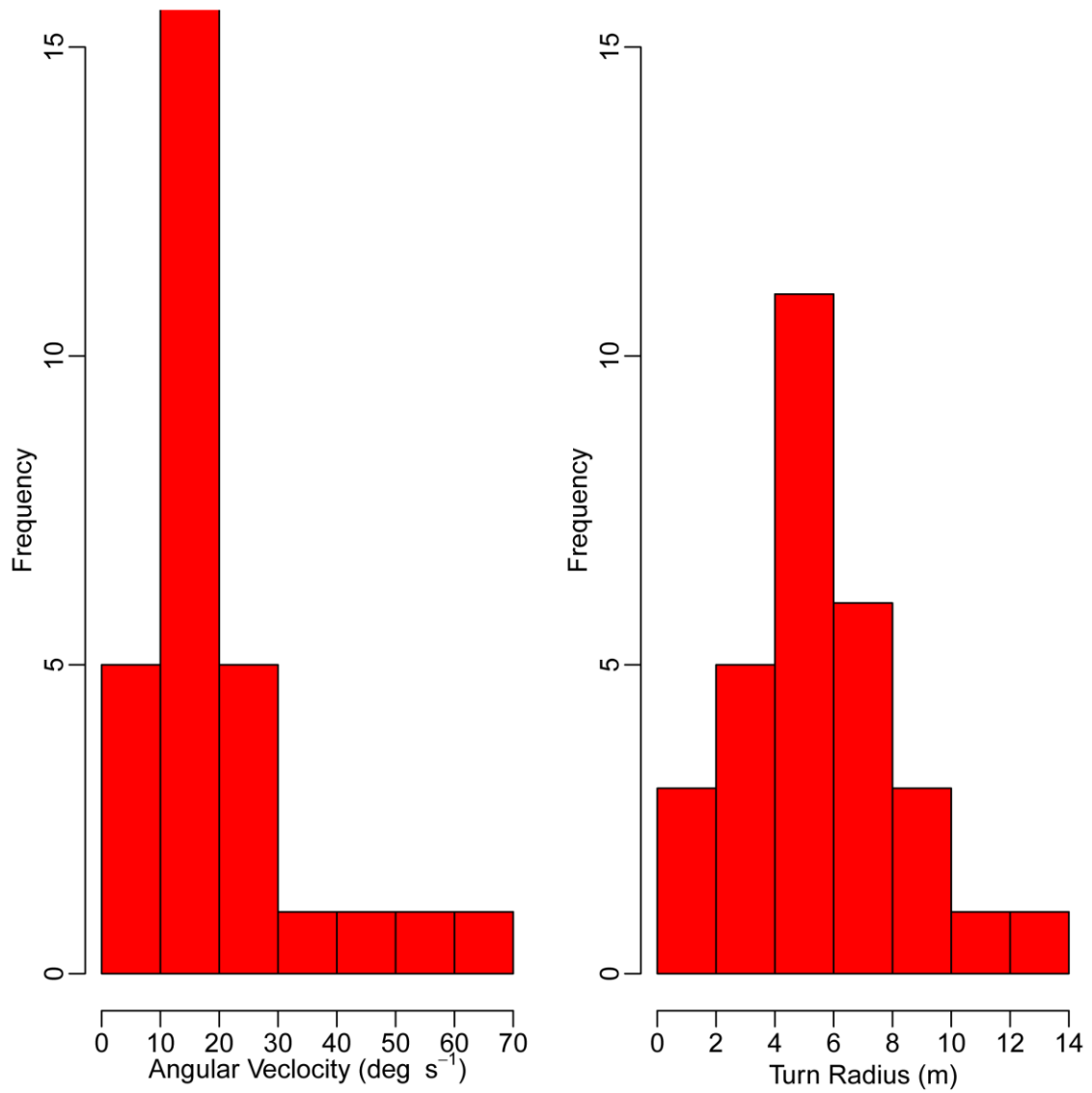
Figure 3. Frequency histograms of the angular velocity, ω, and turning radius, *R,* for each of the 30 turning sequences.
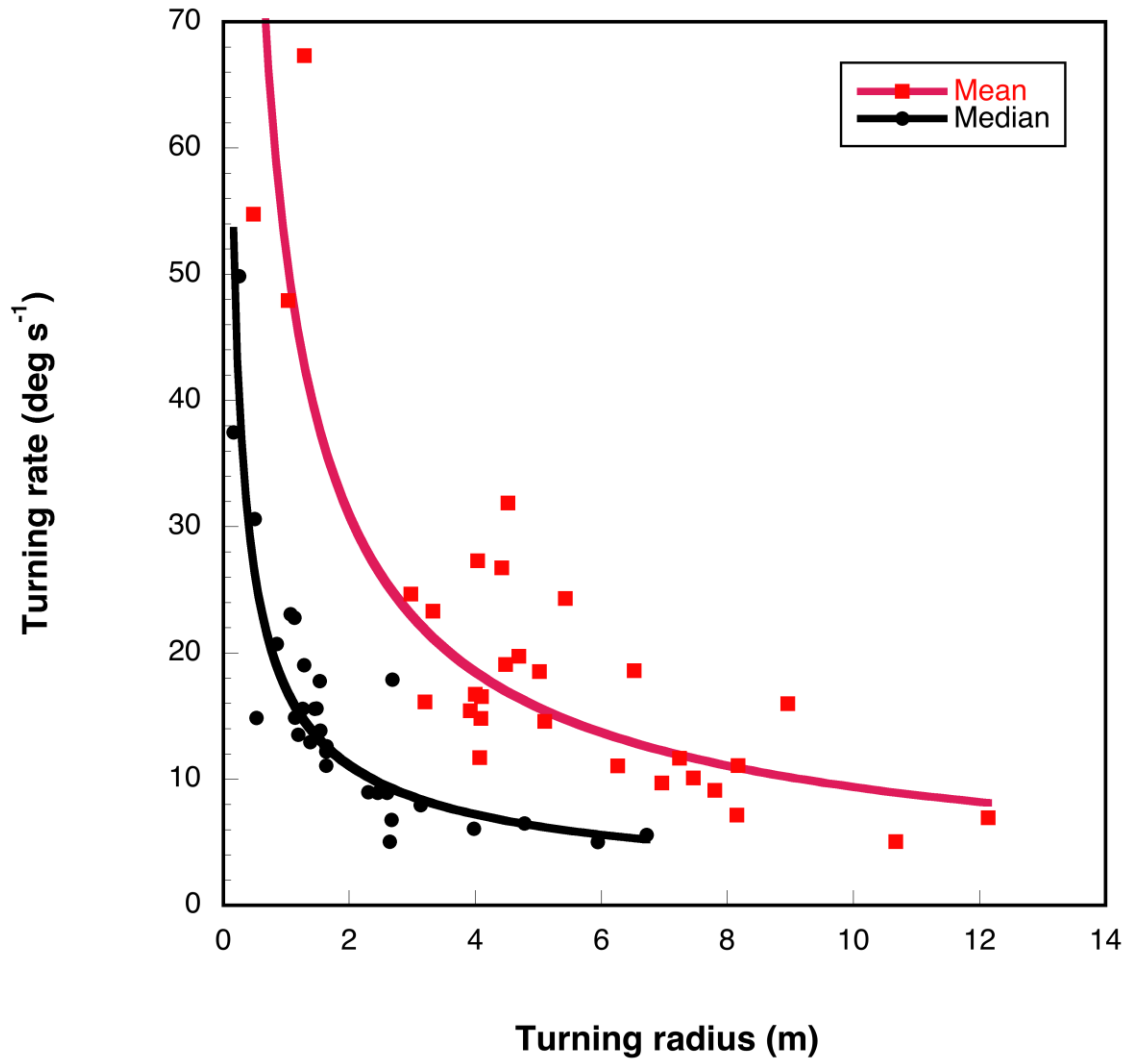
Figure 4. Relationship of mean and median angular velocity, ω, to turning radius, *R*. ω decreased curvilinearly with increasing *R*.
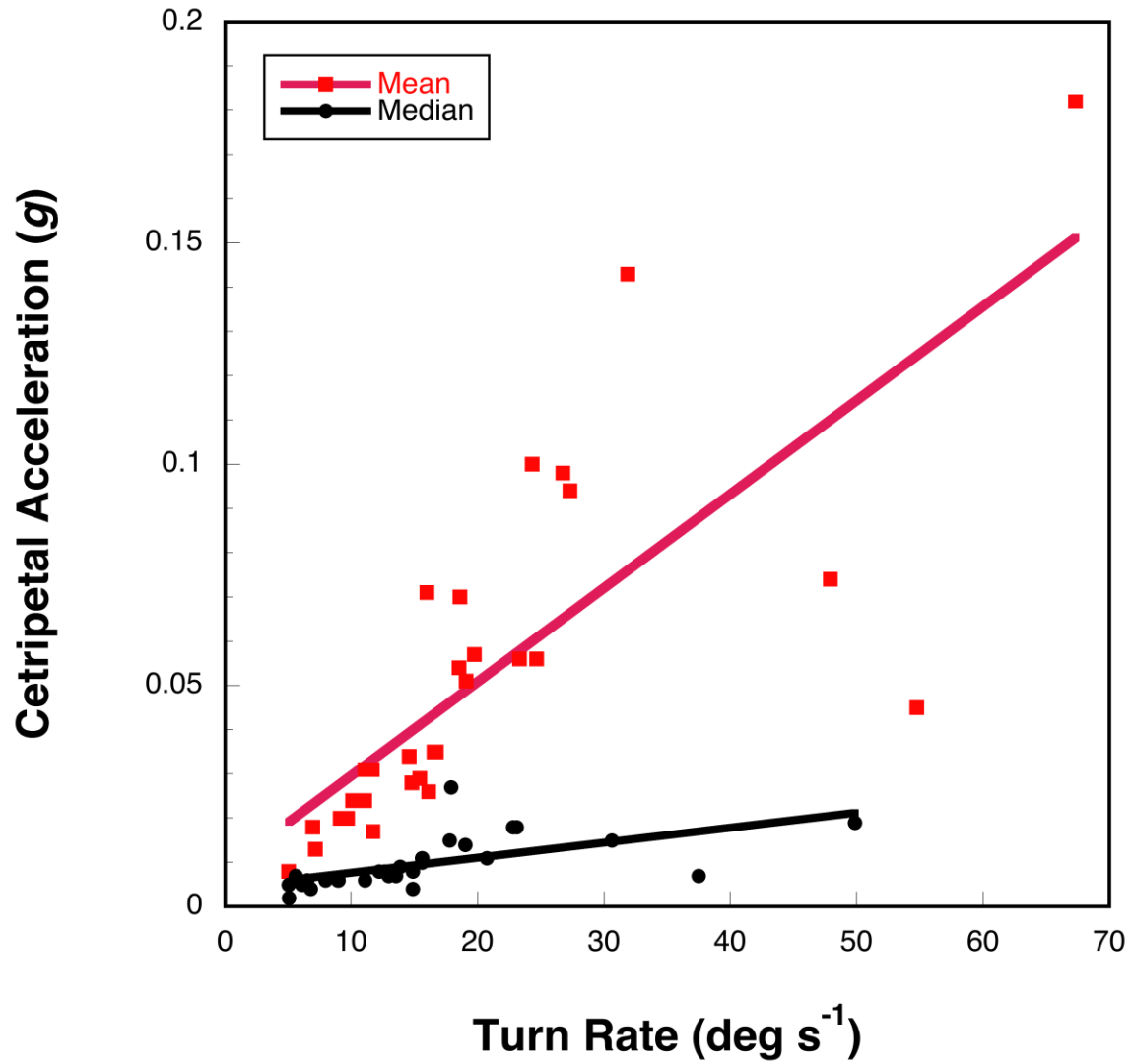
Figure 5. Plot of centripetal acceleration as a function of turn rate for mean and median

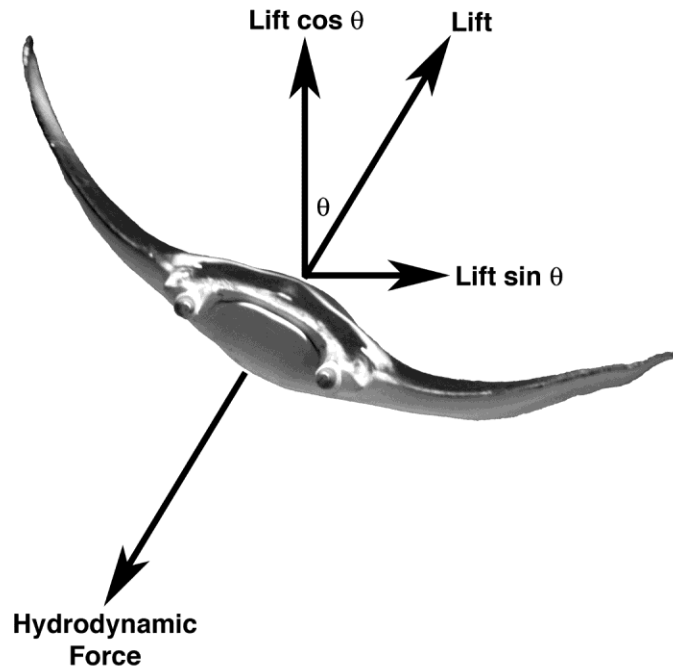values. Only the regression for the mean values was significant.

Figure 6. Frontal view showing the forces acting on a banking manta while executing a turn to the animals left.
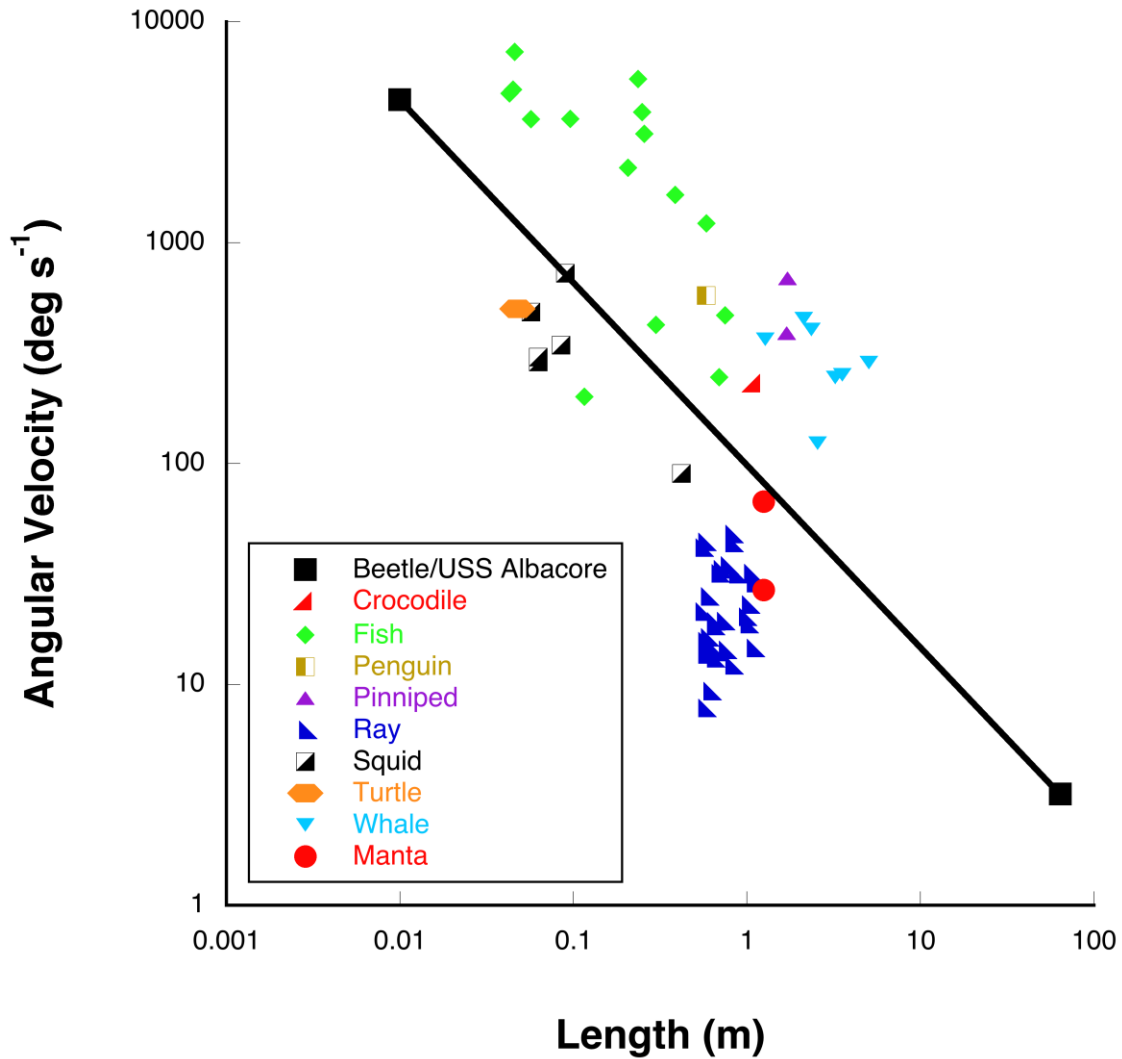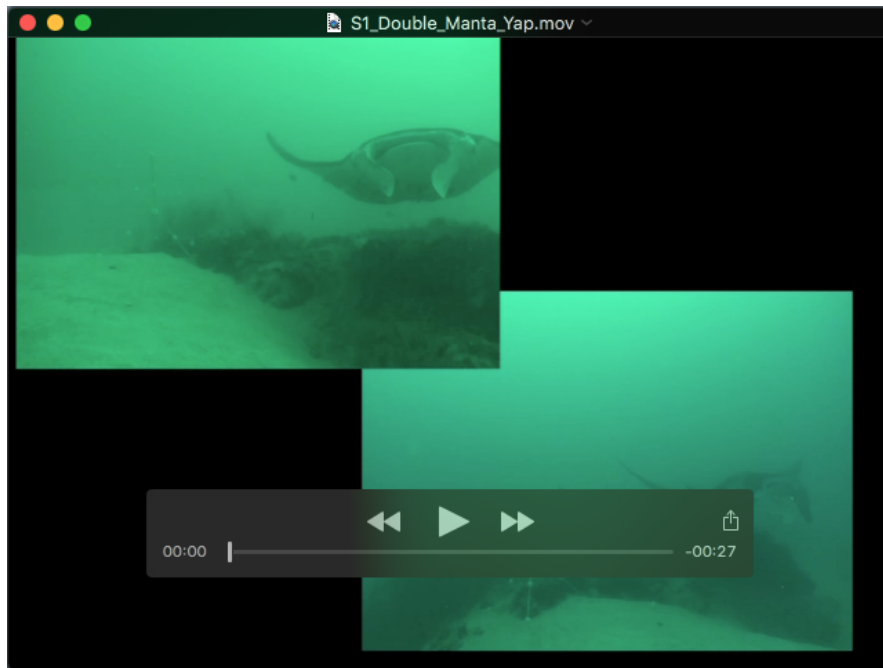
Figure 7. The turning performance of the manta with respect to data for rigid-bodied aquatic animals. Comparison of turning rate, ω, with respect to body size. The line connecting the whirligig beetle and submarine represents a limit to turning performance for rigid bodies and corresponds to ω =99.25 $L^{0.835}$. Symbols above the line represent flexible-bodied animals, whereas symbols below the line are for rigid-bodies. The only fish to have a turning rate below the line was the boxfish, which has a rigid body. The upper point for the manta is the maximum turning rate recorded, whereas the lower point

for the manta represents the lowest turning rate of the highest 20% of the data for the manta. Data from Webb (1976, 1983), Hui (1985), Foyle and O'Dor (1988), Miller (1991), Blake et. al. (1995), Gerstner (1999), Walker (2000), Frey and Salisbury (2001), Fish (1997, 2002), Fish and Nicastro, 2003, Fish et al., 2003, Kajiura et al. (2003), Domenici et al. (2004), Rivera et al. (2006), Parson et al. (2011), Jastrebsky et al. (2016, 2017), Helmer et al. (2016), and Geurten et al. (2017).

Movie S1